RESEARCH ARTICLE

INTERNATIONAL RESEARCH JOURNAL OF MULTIDISCIPLINARY TECHNOVATION

Asian Research Association

DOI: 10.54392/irjmt24112

A Quantum Chemical Investigation on Structural, Spectroscopic and Nonlinear Optical properties of an Organic Molecule Serotonin

R. Thayala Sanker [a, b], S. Arunachalam [c, *], S. Raju [d], M. Velayutham Pillai [e], R. Kumaresan [f]

[a] Department of Chemistry, JCT College of Engineering and Technology, Pichanur, Coimbatore-641105, India

[b] Research and Development Centre, Bharathiar University, Coimbatore-641046, Tamil Nadu, India

[c] Department of Electrochemistry, Saveetha School of Engineering, Saveetha Institute of Medical and Technical Sciences, Chennai-602105, India

[d] Department of Physics, KPR Institute of Engineering and Technology, Coimbatore-641407, Tamil Nadu, India

[e] Post Graduate Department of Chemistry, Nallamuthu Gounder Mahalingam College, Pollachi-642001, Tamil Nadu, India.

[f] Department of Chemistry, Jai Shriram Engineering college, Tirupur-638660, Tamil Nadu, India

*Corresponding Author Email: drarunachalam.s@gmail.com

DOI: https://doi.org/10.54392/irjmt24112

Received: 07-09-2023; Revised: 28-12-2023; Accepted: 13-01-2024; Published: 30-01-2024

Abstract: Serotonin, a neurotransmitter known for promoting feelings of happiness and optimism, was the subject of theoretical studies conducted using Gaussian software. In these experiments, the 6-311++G/B3LYP basis set was employed. The finite-field-based B3LYP/6-311++G (d,p) approach was used to compute the first-order hyper polarizability and associated properties of this chemical system. Additionally, a Natural Bond Orbital (NBO) analysis was conducted to assess the molecule's stability, taking into account hyper conjugative interactions and charge delocalization. Additionally, HOMO-LUMO energy levels were computed to assess whether a chemical exhibits electrophilic or nucleophilic characteristic. TD-DFT simulations were conducted to examine the electrical and optical characteristics of the material, including absorption wavelengths and excitation energy. Subsequently, the chemical compound's electrophilic or nucleophilic nature was determined by calculating the molecular electrostatic potential (MEP).

Keywords: Nonlinear Optics, Serotonin, HOMO-LUMO, TD-DFT

1. Introduction

Serotonin, also referred to as 5-hydroxytryptamine (5-HT) [1, 2], one of the central nervous system's most vital neurotransmitters, it plays a fundamental and diverse role. Operating both as a hormone and a mitogen [2], it actively participates in intracellular signaling [3]. Its impact extends across various facets of daily life and human physiology, assuming a pivotal role in mood regulation, encompassing emotions such as anxiety, sleep, overall well-being, and blood pressure [4]. The influence of 5-HT is truly multifaceted [5]. Tryptophan is utilized in the synthesis of serotonin, which is also referred to as 5-HT, 5-Hydroxytryptamine, Enteramine, Thrombocyte, 3-(β-Aminoethyl)-5-hydroxyindole, and Thrombotonin. Serotonin is produced in serotonergic centers from tryptophan. During this process, it competes for entry through the blood-brain barrier with tyrosine and branched-chain amino acids [6]. Additionally, serotonin serves as a key focus for various medications employed in the treatment of psychiatric conditions such as schizophrenia and depression [7]. Selective serotonin reuptake inhibitors (SSRIs) have proven notably effective in managing conditions such as unipolar depression and bipolar disorders [8]. Ongoing research and historical findings provide compelling evidence supporting the significant role played by serotonergic systems, especially the central 5-HT2A receptors, in the initiation of drug-induced psychotic states and their potential association with the etiology of various psychotic disorders, including schizophrenia [9]. Furthermore, variations in the efficiency of electrical coupling within brain circuits could influence the pharmacological impact of serotonin, a neuromodulatory substance associated with Alzheimer's disease and other neurological disorders [10]. The field of computational quantum chemistry is dynamic and captivating, offering robust tools for computing various characteristics of organic molecules. Some of these characteristics include ground-state geometry, studies of Natural Bond Orbitals (NBO), and evaluations of Non-Linear Optical (NLO) properties [11]. Diverse methods, such as Density Functional Theory (DFT), molecular mechanics, semiempirical approaches, and ab-initio methods, are frequently employed to compute these

molecular properties. Past computational studies on serotonin have encompassed a wide array of investigations, including the analysis of its electronic structure using Gaussian 09 and Turbopole, optimization using methods like DFT-B3LYP, B3PW91, X3LYP, TPSSh, M05, M06, M05-2X, M06-2X, MP2, and HF [12, 13]. These studies have probed into spectroscopic signatures [13], energy optimization, Raman vibrational frequencies [12], mathematical modeling of serotonergic signaling [6], gas-phase analysis using DFT-M06-2X, and the determination of free activation energy [13]. Researchers have also explored steady-state variable values and conducted neurobiological computational studies, scrutinizing the activity patterns of the thalamus in conditions such as dystonia and Parkinson's disease [14]. Furthermore, this research has encompassed 3D-QSAR experiments, which involved CoMFA and CoMSIA analyses, conducted using SYBYL-X-2.1.1. Additionally, it involved ADME analysis using Swiss ADME, as well as molecular docking conducted with Schrodinger software [15, 16]. In this research endeavor, our aim is to analyze the serotonin compound comprehensively, including geometric optimization, nonlinear optical studies, HOMO-LUMO investigations, and NBO analysis.

2. Computational Details

Our primary computational tool for this undertaking is Gaussian09 software [17]. When applying the B3LYP functional level of theory, the initial step involves conducting geometric optimization with the 6-311++G basis set. Subsequently, we will visualize the optimized molecular structure using ChemCraft software. The experimentally synthesized crystal structure will undergo analysis using Mercury 2.0 software [18]. For investigating the molecule's HOMO-LUMO (Higher Occupied Molecular Orbital-Lower Unoccupied Molecular Orbital) characteristics [17, 18], we will utilize the GaussView 5.0 program. Additionally, Gaussian 09 software with the B3LYP-6-311++G basis set will be employed to perform a Natural Bond Orbital (NBO) analysis [19]. To determine Non-Linear Optical (NLO) parameters such as Dipole Moment, Hyper Polarizability, and Anisotropy of Polarizability, we will use the DFT (B3LYP)-6-311++G basis set [17, 20]. To examine UV-Vis spectra and elucidate the electronic characteristics [7, 21, 22], we will employ the TD-DFT (B3LYP/6-311++G) Method. Additionally, we will create and display Mapped Electrostatic Potential (MESP) and Total Electron Density (TED) surfaces using GaussView 05 software [17, 23], potentially yielding further insights.

3. Result and Discussion

3.1 Geometrical Optimization

The arrangement of the ethylamine side chain and hydroxyl group is pivotal in establishing the structural arrangements available to serotonin [4]. In Figure 1, we have illustrated the molecular structure of serotonin and calculated its optimal values for parameters such as bond distances, bond angles, and torsion angles. These optimized parameters are detailed in Table 1. Serotonin comprises 25 atoms, each participating in the formation of various bond types, including O-C, O-H, N-C, N-H, C-C, and C-H, with each type characterized by specific bond distances.

For instance, bonds like C-O-H, C-N-C, C-N-H, H-N-H, C-C-C, C-C-H, H-C-H, N-C-C, N-C-H, C-C-H, O-C-C, among others, involve bond angles. Similarly, bonds like H-O-C-C, C-N-C-C, H-N-C-C, C-N-C-H, H-N-C-H, C-C-C-C, C-C-C-H, C-C-C-N, H-C-C-N, H-C-C-H, N-C-C-C, N-C-C-H, H-C-C-O, H-C-C-C, O-C-C-C, O-C-C-H, C-C-C-H, have torsion angles, which represent the angle between four atoms in the bond.

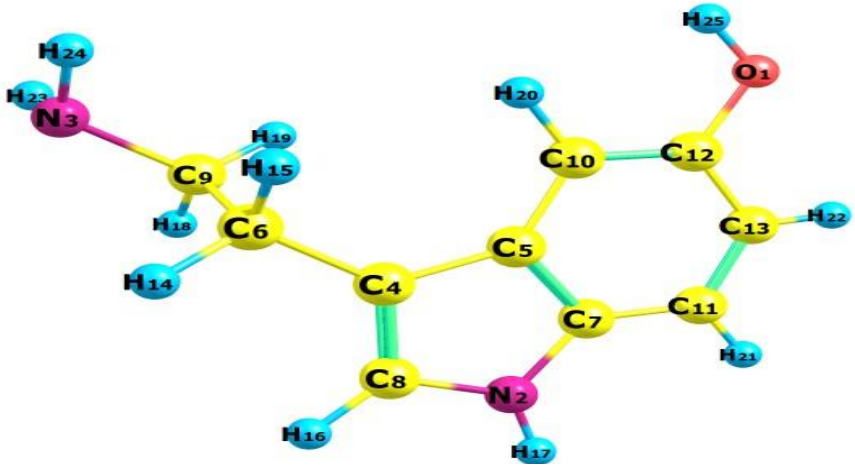

Figure 1. The Optimized Stucture of Serotonin

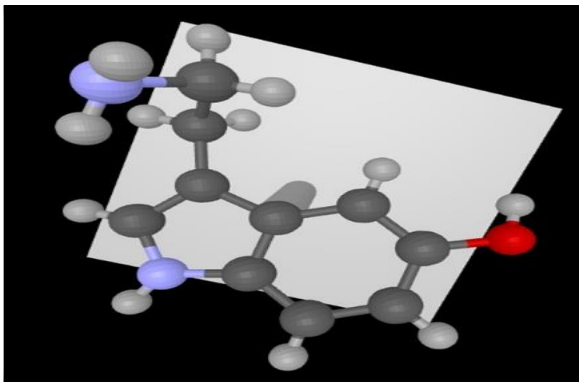

Figure 2. The Experimentally synthesized serotonin 3D-Visiualized picture from Mercury

Table 1. The optimized parameters of theoretically and experimentally synthesized Serotonin

Angstroms and Degrees			
	Atomic Bond	**Theoretical**	**Experimental**
Bond Length			
1	O1-C12	1.3775	1.376
2	O_1-H_{25}	0.9623	0.883
3	N_2-C_7	1.3821	1.376
4	N_2-C_8	1.3806	1.372
5	N_2-H_{17}	1.0055	0.878
6	N_3-C_9	1.4686	1.473
7	N_3-H_{23}	1.0145	0.894
8	N_3-H_{24}	1.0156	0.915
9	C_4-C_5	1.4417	1.438
10	C_4-C_6	1.501	1.501
11	C_4-C_8	1.3733	1.358
12	C_5-C_7	1.4181	1.413
13	C_5-C_{10}	1.4075	1.399
14	C_6-C_9	1.5371	1.518
15	C_6-H_{14}	1.0938	0.970
16	C_6-H_{15}	1.0983	0.970
17	C_7-C_{11}	1.3962	1.390
18	C_8-H_{16}	1.0796	0.930
19	C_9-H_{18}	1.0939	0.970
20	C_9-H_{19}	1.1006	0.970
21	C_{10}-C_{12}	1.3865	1.377
22	C_{10}-H_{20}	1.0863	0.930
23	C_{11}-C_{13}	1.3859	1.376
24	C_{11}-H_{21}	1.0845	0.930

25	C_{12}-C_{13}	1.4088	1.406
26	C_{13}-H_{22}	1.0829	0.930
Bond angles			
1	C_{12}-O_1-H_{25}	109.4291	109.45
2	C_7-N_2-C_8	108.9594	108.64
3	C_7-N_2-H_{17}	125.6745	126.35
4	C_8-N_2-H_{17}	125.3484	124.80
5	C_9-N_3-H_{23}	111.0722	109.28
6	C_9-N_3-H_{24}	110.9607	108.81
7	H_{23}-N_3-H_{24}	107.0709	113.22
8	C_5-C_4-C_6	127.3781	25.98
9	C_5-C_4-C_8	106.1647	106.33
10	C_6-C_4-C_8	126.452	127.65
11	C_4-C_5-C_7	107.4103	106.97
12	C_4-C_5-C_{10}	133.6042	133.73
13	C_7-C_5-C_{10}	118.981	119.28
14	C_4-C_6-C_9	113.7663	112.92
15	C_4-C_6-H_{14}	110.2151	108.97
16	C_4-C_6-H_{15}	109.5875	108.98
17	C_9-C_6-H_{14}	108.1471	109.03
18	C_9-C_6-H_{15}	108.6915	109.04
19	H_{14}-C_6-H_{15}	106.1373	107.77
20	N_2-C_7-C_5	107.2174	107.41
21	N_2-C_7-C_{11}	130.8837	131.08
22	C_5-C_7-C_{11}	121.8978	121.50
23	N_2-C_8-C_4	110.2474	110.65
24	N_2-C_8-H_{16}	120.5364	124.67
25	C_4-C_8-H_{16}	129.2151	124.68
26	N_3-C_9-C_6	110.3456	111.20
27	N_3-C_9-H_{18}	107.8727	109.39
28	N_3-C_9-H_{19}	113.6517	109.37
29	C_6-C_9-H_{18}	108.7859	109.43
30	C_6-C_9-H_{19}	109.3289	109.40
31	H_{18}-C_9-H_{19}	106.6842	107.98
32	C_5-C_{10}-C_{12}	118.8796	119.00
33	C_5-C_{10}-H_{20}	120.7769	120.51
34	C_{12}-C_{10}-H_{20}	120.3435	120.49
35	C_7-C_{11}-C_{13}	118.17	118.09
36	C_7-C_{11}-H_{21}	121.4812	120.97
37	C_{13}-C_{11}-H_{21}	120.3487	120.94

38	O_1-C_{12}-C_{10}	122.603	122.27
39	O_1-C_{12}-C_{13}	116.0247	116.83
40	C_{10}-C_{12}-C_{13}	121.3723	120.89
41	C_{11}-C_{13}-C_{12}	120.6988	121.13
42	C_{11}-C_{13}-H_{22}	120.9104	119.47
43	C_{12}-C_{13}-H_{22}	118.3907	119.40
Torsion angles			
1	H_{25}-O_1-C_{12}-C_{10}	0.5748	-13.85
2	H_{25}-O_1-C_{12}-C_{13}	-179.4603	165.42
3	C_8-N_2-C_7-C_5	-0.2387	-0.66
4	C_8-N_2-C_7-C_{11}	179.3683	178.22
5	H_{17}-N_2-C_7-C_5	-178.7743	174.40
6	H_{17}-N_2-C_7-C_{11}	0.8327	-6.73
7	C_7-N_2-C_8-C_4	0.2844	0.31
8	C_7-N_2-C_8-H_{16}	-179.3778	-179.71
9	H_{17}-N_2-C_8-C_4	178.8259	-174.84
10	H_{17}-N_2-C_8-H_{16}	-0.8363	5.15
11	H_{23}-N_3-C_9-C_6	-174.0744	28.87
12	H_{23}-N_3-C_9-H_{18}	5.3595	-92.11
13	H_{23}-N_3-C_9-H_{19}	62.7101	149.81
14	H_{24}-N_3-C_9-C_6	66.9466	152.95
15	H_{24}-N_3-C_9-H_{18}	-174.3385	31.97
16	H_{24}-N_3-C_9-H_{19}	6.2689	-86.11
17	C_6-C_4-C_5-C_7	-179.1543	175.88
18	C_6-C_4-C_5-C_{10}	1.6462	-4.41
19	C_8-C_4-C_5-C_7	0.0569	-0.56
20	C_8-C_4-C_5-C_{10}	-179.1425	177.94
21	C_5-C_4-C_6-C_9	77.1113	-64.14
22	C_5-C_4-C_6-H_{14}	-161.2335	174.54
23	C_5-C_4-C_6-H_{15}	-44.7841	57.19
24	C_8-C_4-C_6-C_9	-101.9468	-125.66
25	C_8-C_4-C_6-H_{14}	19.7083	-8.30
26	C_8-C_4-C_6-H_{15}	136.1577	-125.66
27	C_5-C_4-C_8-N_2	-0.2069	0.16
28	C_5-C_4-C_8-H_{16}	179.4176	-179.82
29	C_6-C_4-C_8-N_2	179.0138	-177.44
30	C_6-C_4-C_8-H_{16}	-1.3617	2.58
31	C_4-C_5-C_7-N_2	0.1108	0.74
32	C_4-C_5-C_7-C_{11}	-179.5392	-178.26
33	C_{10}-C_5-C_7-N_2	179.4482	-178.01

34	C_{10}-C_5-C_7-C_{11}	-0.2019	2.99
35	C_4-C_5-C_{10}-C_{12}	179.2235	-178.95
36	C_4-C_5-C_{10}-H_{20}	-0.6893	1.10
37	C_7-C_5-C_{10}-C_{12}	0.0967	-0.61
38	C_7-C_5-C_{10}-H_{20}	-179.8161	179.45
39	C_4-C_6-C_9-N_3	179.6023	-61.92
40	C_4-C_6-C_9-H_{18}	61.4461	59.04
41	C_4-C_6-C_9-H_{19}	4.701	177.16
42	H_{14}-C_6-C_9-N_3	56.8059	59.36
43	H_{14}-C_6-C_9-H_{18}	-1.3503	-179.68
44	H_{14}-C_6-C_9-H_{19}	-177.4975	-61.55
45	H_{15}-C_6-C_9-N_3	8.0073	176.79
46	H_{15}-C_6-C_9-H_{18}	-176.1635	-62.25
47	H_{15}-C_6-C_9-H_{19}	67.6894	55.87
48	N_2-C_7-C_{11}-C_{13}	-179.467	178.81
49	N_2-C_7-C_{11}-H_{21}	0.441	-1.17
50	C_5-C_7-C_{11}-C_{13}	0.0909	-2.45
51	C_5-C_7-C_{11}-H_{21}	-180.0012	177.57
52	C_5-C_{10}-C_{12}-O_1	-179.9247	177.05
53	C_5-C_{10}-C_{12}-C_{13}	0.1122	-2.19
54	H_{20}-C_{10}-C_{12}-O_1	-0.0115	-3.01
55	H_{20}-C_{10}-C_{12}-C_{13}	-179.9745	177.75
56	C_7-C_{11}-C_{13}-C_{12}	0.1218	-0.40
57	C_7-C_{11}-C_{13}-H_{22}	179.976	179.52
58	H_{21}-C_{11}-C_{13}-C_{12}	-179.7872	179.58
59	H_{21}-C_{11}-C_{13}-H_{22}	0.067	-0.50
60	O_1-C_{12}-C_{13}-C_{11}	179.8072	-176.52
61	O_1-C_{12}-C_{13}-H_{22}	-0.0507	3.56
62	C_{10}-C_{12}-C_{13}-C_{11}	-0.2275	2.76
63	C_{10}-C_{12}-C_{13}-H_{22}	179.9147	-177.16

Upon closer examination, it's evident that bonds like O1-C12, N3-C9, C4-C6, C5-C10, C12-C13 exhibit nearly identical distance values in both theoretical and experimental computations, measuring at 1.37Å, 1.47Å, 1.50Å, 1.40Å, and 1.40Å, respectively. The longest distance is observed in the C6-C9 bond, with theoretical and experimental measurements of 1.537Å and 1.518Å, respectively. Furthermore, the highest bond angle is found in the C4-C5-C10 bond, measuring 133.6 degrees and 133.7 degrees in the theoretical and experiment data, respectively. Lastly, the most pronounced torsion angle is evident in the theoretical H7-C11-C13-H22 bond, registering at 179.9 degrees, While the experimental counterpart, H21-C11-C13-C12, records a value of 179.58 degrees.

3.2 HOMO-LUMO Analysis

Frontier Molecular Orbital (FMO) is the encompassing term that includes HOMO-LUMO (Higher Occupied Molecular Orbital and Lower Unoccupied Molecular Orbital) [24]. The HOMO denotes the capacity to donate an electron, while the LUMO represents the ability to accept an electron as an electron acceptor. The significance of HOMO and LUMO in governing chemical processes was originally recognized by scientist Fukui [25].

Table 2. The computed energy gap values for significant orbital energy transitions

S.No	Molecular Orbital	Energy value	Energy Gap	
			Molecular Orbital Energy Transitions	Energy gap Value (eV)
1	HOMO	8.6741	HOMO→LUMO	3.4558
2	HOMO-1	9.0170	HOMO -1→LUMO	3.7987
3	HOMO-2	9.7930	HOMO -2 →LUMO	4.5742
4	LUMO	5.2183	HOMO→LUMO+1	4.8653
5	LUMO+1	3.8087	HOMO -1 →LUMO+1	5.2082
6	LUMO+2	3.2136	HOMO-2→LUMO+1	5.9843
			HOMO→LUMO+2	5.4604
			HOMO-1→LUMO+2	5.8033
			HOMO-2→LUMO+2	6.5794

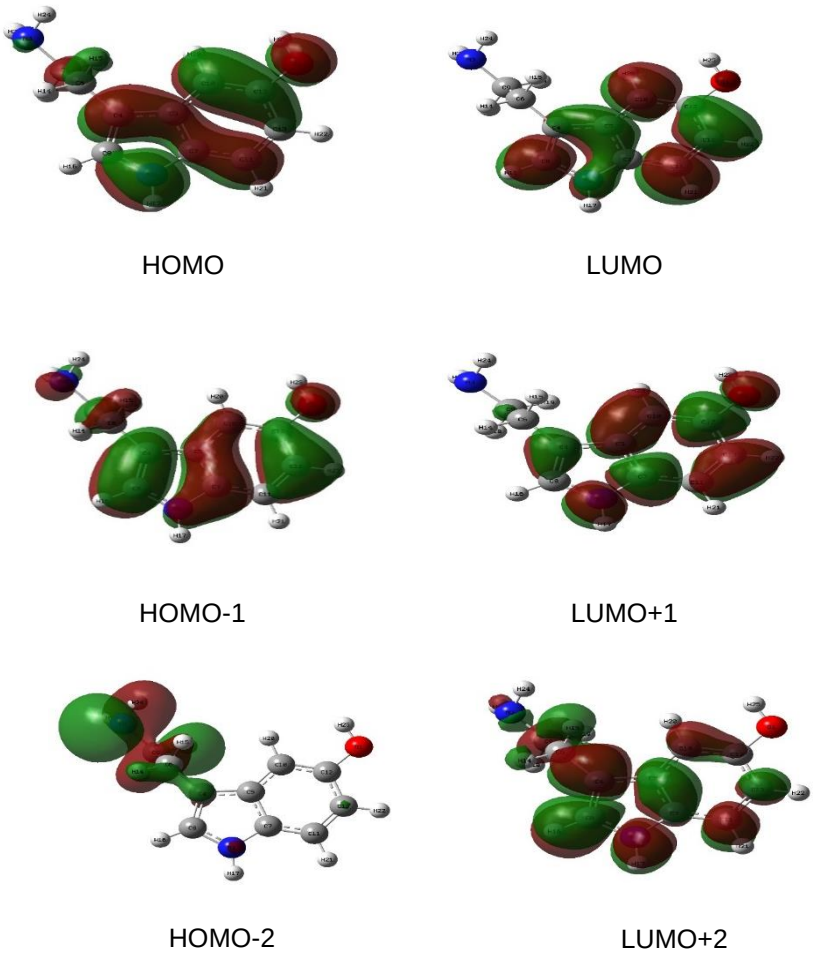

Figure 3. FMO Diagram

In visual representations, shown in Figure 3, the positive region is typically represented in red, while the negative region is depicted in green. The energy difference between HOMO and LUMO helps reveal the charge transfer interactions occurring within the molecule. Importantly, each compound exhibits a substantial transfer of charge from HOMO to LUMO, along with a reduction in energy level. This observation implies that these substances may serve as promising candidates for a variety of nonlinear optical (NLO) applications [26].

The energy difference between serotonin's HOMO and LUMO orbitals stands at 3.4558 eV. Notably, there is a larger band gap between HOMO-2 and LUMO+2, measuring 6.5794 eV. This substantial gap serves as evidence of charge transfer taking place within the molecule.

A larger energy gap implies higher kinetic stability when compared to a smaller one. Furthermore, a molecule with a higher energy gap typically exhibits lower chemical reactivity [27]. The computed energy gap values for significant orbital energy transitions are presented in Table 2.

3.3 NBO Analysis

Natural Bond Orbital Analysis is a potent method for investigating both intra- and intermolecular bonding, as well as interactions between bonds. It offers a valuable framework for the examination of conjugative interactions or charge transfer within molecular systems [28]. The NBO analysis employs the second-order Fock matrix to evaluate interactions between donors and acceptors. These interactions result in the transfer of electron occupancy from unoccupied non-Lewis orbitals to localized NBOs within the idealized Lewis structure [29].

The stabilization energy (E(2)) linked to the delocalization from each donor (i) to acceptor (j) is calculated as follows:

$$E(2) = \Delta Eij = qi \frac{F(i,j)^2}{\varepsilon_j - \varepsilon_i}$$

In this context, several key elements come into play: qi represents the donor orbital occupancy, while i and j refer to the diagonal elements, and F(i, j) stands for the off-diagonal NBO Fock matrix element [30,31]. It's important to note that the magnitude of the E(2) value gauges the strength of interactions between electron donors and acceptors. To put it simply, a larger E(2) value indicates a heightened degree of conjugation throughout the system and a more pronounced tendency for electron donation from donors to acceptors [32].

Molecules have undergone comprehensive NBO analysis at the DFT/6-311++G(d,p) level, and the results are presented in Table 3.

Table 3 NBO Analysis with stabilization energy values

Donor (i)	Type	Occupancy	Acceptor	Type	Occupancy	E(2)	E(j)-E(i)	F(i,j)
O1 - C12	σ	1.9942	C 5 - C 10	σ*	0.02254	1.28	1.45	0.039
			C 10 - C 12	σ*	0.02482	0.85	1.47	0.032
			C 11 - C 13	σ*	0.01076	1.32	1.49	0.04
			C 12 - C 13	σ*	0.02457	1.08	1.48	0.036
			C 13 - H 22	σ*	0.01131	2.59	2.9	0.077
			C 11 - C 13	σ*	0.01076	1.32	1.49	0.04
			C 12 - C 13	σ*	0.02457	1.08	1.48	0.036
			C 13 - H 22	σ*	0.01131	2.59	2.9	0.077
O 1 - H 25	σ	1.98754	C 12 - C 13	σ*	0.02457	6.14	1.32	0.08
			C 13 - H 22	σ*	0.01131	6.64	2.74	0.12
			C 12 - C 13	σ*	0.02457	6.14	1.32	0.08
N 2 - C 7	σ	1.98562	C 13 - H 22	σ*	0.01131	6.64	2.74	0.12
			N 2 - C 8	σ*	0.01215	1.43	1.24	0.038
			N 2 - H 17	σ*	0.01674	0.77	1.19	0.027
			C 5 - C 7	σ*	0.02689	1.18	1.35	0.036
			C 5 - C 10	σ*	0.02254	2.34	1.36	0.05
			C 7 - C 11	σ*	0.02148	2.2	1.38	0.049
			C 8 - H 16	σ*	0.01328	2.24	1.22	0.047
			C 11 - C 13	σ*	0.01076	0.79	1.4	0.03
			C 13 - H 22	σ*	0.01131	1.26	2.8	0.053

N 2 - C 8	σ	1.98487	N 2 - C 7	σ*	0.02554	1.72	1.25	0.041
			N 2 - H 17	σ*	0.01674	0.69	1.19	0.026
			C 4 - C 6	σ*	0.01967	3.85	1.24	0.062
			C 4 - C 8	σ*	0.01659	1.23	1.4	0.037
			C 7 - C 11	σ*	0.02148	4.36	1.37	0.069
			C 4 - C 8	σ*	0.01659	1.17	1.29	0.035
			C 5 - C 7	σ*	0.02689	1.79	1.24	0.042
N 2 - H 17	σ	1.99056	C 4 - C 6	σ*	0.01967	1.58	1.16	0.038
			C 6 - C 9	σ*	0.02272	2.33	1	0.043
N 3 - C 9	σ	1.99315	C 9 - H 18	σ*	0.0175	0.54	1.01	0.021
N 3 - H 23	σ	1.98947	C 9 - H 18	σ*	0.0175	2.08	1.01	0.041
			C 13 - H 22	σ*	0.01131	3.17	2.61	0.081
N 3 - H 24	σ	1.99044	N 2 - C 7	σ*	0.02554	0.94	1.09	0.029
			N 2 - C 8	σ*	0.01215	1.07	1.08	0.031
			C 4 - C 6	σ*	0.01967	2.11	1.08	0.043
			C 4 - C 8	σ*	0.01659	2.43	1.24	0.049
C 4 - C 5	σ	1.9638	C 5 - C 7	σ*	0.02689	2.38	1.19	0.048
			C 5 - C 10	σ*	0.02254	4.32	1.2	0.064
			C 6 - H 14	σ*	0.01319	0.69	1.05	0.024
			C 7 - C 11	σ*	0.02148	3.69	1.21	0.06
			C 8 - H 16	σ*	0.01328	4.66	1.06	0.063
			C 10 - C 12	σ*	0.02482	1.16	1.22	0.034
			C 13 - H 22	σ*	0.01131	3.86	2.64	0.091
			N 2 - C 8	σ*	0.01215	1.38	1.07	0.034
			N 3 - C 9	σ*	0.00868	1.8	0.98	0.038
			C 4 - C 5	σ*	0.02881	2.65	1.16	0.05
			C 4 - C 8	σ*	0.01659	2.97	1.23	0.054
C 4 - C 6	σ	1.97725	C 5 - C 7	σ*	0.02689	1.31	1.18	0.035
			C 6 - C 9	σ*	0.02272	0.76	1.01	0.025
			C 6 - H 14	σ*	0.01319	0.55	1.04	0.021
			C 6 - H 15	σ*	0.01877	0.56	1.02	0.021
			N 2 - C 8	σ*	0.01215	1.01	1.15	0.03
			N 2 - H 17	σ*	0.01674	3.29	1.09	0.054
			C 4 - C 5	σ*	0.02881	2.56	1.24	0.05
			C 4 - C 6	σ*	0.01967	2.61	1.15	0.049
			C 5 - C 10	σ*	0.02254	5.29	1.26	0.073
C 4 - C 8	σ	1.97347	C 8 - H 16	σ*	0.01328	1.8	1.12	0.04
			C 4 - C 8	π*	0.30572	1.51	0.29	0.02
			C 5 - C 7	π*	0.49624	16.74	0.29	0.068
			C 6 - C 9	σ*	0.02272	3.62	0.64	0.044
			C 6 - H 15	σ*	0.01877	2.11	0.65	0.034
			C 13 - H 22	σ*	0.01131	2.08	2.26	0.064
	π		N 2 - C 7	σ*	0.02554	0.98	1.1	0.029
			N 2 - H 17	σ*	0.01674	4.08	1.04	0.059
C 5 - C 7	σ	1.95794	C 4 - C 5	σ*	0.02881	2.38	1.19	0.048
			C 4 - C 6	σ*	0.01967	4.74	1.1	0.065
			C 5 - C 10	σ*	0.02254	3.1	1.21	0.055

			C 7 - C 11	σ*	0.02148	4.51	1.23	0.067
			C 10 - H 20	σ*	0.01473	2.79	1.08	0.049
			C 11 - H 21	σ*	0.01354	3.52	1.11	0.056
			C 13 - H 22	σ*	0.01131	3.02	2.65	0.081
			C 4 - C 8	π*	0.30572	18.51	0.28	0.065
			C 10 - C 12	π*	0.36373	17.91	0.27	0.063
			C 11 - C 13	π*	0.33502	20.93	0.27	0.068
C 5 - C 10	σ	1.96953	O 1 - C 12	σ*	0.02346	4.26	1.03	0.059
			N 2 - C 7	σ*	0.02554	1.68	1.14	0.039
			C 4 - C 5	σ*	0.02881	4.52	1.22	0.066
			C 4 - C 8	σ*	0.01659	0.7	1.29	0.027
			C 5 - C 7	σ*	0.02689	3.47	1.24	0.058
			C 10 - C 12	σ*	0.02482	3.43	1.26	0.059
			C 10 - H 20	σ*	0.01473	1.39	1.11	0.035
C 6 - C 9	σ	1.97649	N 3 - H 23	σ*	0.00517	1.79	1.03	0.038
			C 4 - C 6	σ*	0.01967	1.09	1.04	0.03
			C 4 - C 8	σ*	0.01659	1.01	1.2	0.031
			C 4 - C 8	π*	0.30572	2.59	0.63	0.039
			C 13 - H 22	σ*	0.01131	1.16	2.59	0.049
C 6 - H 14	σ	1.9782	C 4 - C 5	σ*	0.02881	4.88	1.02	0.063
			C 9 - H 19	σ*	0.03149	2.57	0.88	0.042
C 6 - H 15	σ	1.97402	C 4 - C 8	σ*	0.01659	3.35	1.07	0.054
			C 4 - C 8	π*	0.30572	2.34	0.51	0.033
			C 9 - H 18	σ*	0.0175	2.55	0.87	0.042
			C 11 - H 21	σ*	0.01354	0.52	0.93	0.02
			C 13 - H 22	σ*	0.01131	12.68	2.47	0.159
C 7 - C 11	σ	1.97589	N 2 - C 7	σ*	0.02554	2.23	1.15	0.045
			N 2 - C 8	σ*	0.01215	1.47	1.14	0.037
			C 4 - C 5	σ*	0.02881	1.42	1.23	0.037
			C 5 - C 7	σ*	0.02689	4.6	1.24	0.068
			C 11 - C 13	σ*	0.01076	2.71	1.29	0.053
			C 13 - H 22	σ*	0.01131	2.78	2.7	0.078
C 8 - H 16	σ	1.98486	N 2 - C 7	σ*	0.02554	2.68	1	0.046
			C 4 - C 5	σ*	0.02881	2.31	1.08	0.045
			C 4 - C 8	σ*	0.01659	1.88	1.15	0.041
			C 13 - H 22	σ*	0.01131	4.51	2.54	0.096
C 9 - H 18	σ	1.97901	N 3 - H 24	σ*	0.00885	3.25	0.92	0.049
			C 6 - H 15	σ*	0.01877	2.75	0.89	0.044
C 9 - H 19	σ	1.98702	C 6 - H 14	σ*	0.01319	2.53	0.89	0.042
			C 11 - H 21	σ*	0.01354	0.59	0.94	0.021
			C 12 - C 13	σ*	0.02457	0.55	1.06	0.022
			C 13 - H 22	σ*	0.01131	13.67	2.48	0.164

C 10 - C 12	σ	1.97692	C 4 - C 5	σ*	0.02881	4.13	1.24	0.064
			C 5 - C 10	σ*	0.02254	3.69	1.26	0.061
			C 10 - H 20	σ*	0.01473	1.23	1.13	0.033
			C 12 - C 13	σ*	0.02457	4.23	1.29	0.066
			C 13 - H 22	σ*	0.01131	0.9	2.71	0.044
	π	1.73321	C 5 - C 7	π*	0.49624	18.46	0.29	0.07
			C 11 - C 13	π*	0.33502	16.07	0.29	0.062
C 10 - H 20	σ	1.97732	O 1 - C 12	σ*	0.02346	0.81	0.86	0.024
			C 5 - C 7	σ*	0.02689	3.86	1.07	0.057
			C 5 - C 10	σ*	0.02254	1.12	1.08	0.031
			C 10 - C 12	σ*	0.02482	0.77	1.1	0.026
			C 12 - C 13	σ*	0.02457	3.93	1.1	0.059
C 11 - C 13	σ	1.97284	O 1 - C 12	σ*	0.02346	3.2	1.04	0.052
			N 2 - C 7	σ*	0.02554	5.96	1.15	0.074
			C 7 - C 11	σ*	0.02148	3.4	1.27	0.059
			C 11 - H 21	σ*	0.01354	1.03	1.16	0.031
			C 12 - C 13	σ*	0.02457	2.54	1.28	0.051
	π	1.75607	C 5 - C 7	π*	0.49624	16.63	0.29	0.066
			C 10 - C 12	π*	0.36373	19.22	0.29	0.068
C 11 - H 21	σ	1.97949	C 5 - C 7	σ*	0.02689	4.15	1.07	0.06
			C 7 - C 11	σ*	0.02148	0.65	1.1	0.024
			C 11 - C 13	σ*	0.01076	0.93	1.12	0.029
			C 12 - C 13	σ*	0.02457	3.22	1.1	0.053
C 12 - C 13	σ	1.97277	O 1 - H 25	σ*	0.00703	1.58	1.09	0.037
			C 10 - C 12	σ*	0.02482	3.93	1.26	0.063
			C 10 - H 20	σ*	0.01473	2.52	1.11	0.047
			C 11 - C 13	σ*	0.01076	2.56	1.28	0.051
			C 11 - H 21	σ*	0.01354	2.48	1.15	0.048
C 13 - H 22	σ	1.97796	O 1 - C 12	σ*	0.02346	1.01	0.85	0.026
			C 7 - C 11	σ*	0.02148	3.31	1.09	0.054
			C 10 - C 12	σ*	0.02482	4.07	1.09	0.059
			C 11 - C 13	σ*	0.01076	0.85	1.11	0.027
C 4- C 8	π*	0.30572	C 6 - C 9	σ*	0.02272	1.44	0.35	0.049
			C 6 - H 15	σ*	0.01877	0.68	0.36	0.035

The theoretical results, as presented in Table 3, reveal various types of interactions, including σ→ σ*, σ→ π*, π→ σ*, π→ π*, and π→ σ. Among these interactions, the three highest stabilization energy values are 20.93 kJ mol-1, 18.51 kJ mol-1, and 17.91 kJ mol-1, attributed to the bonding acceptor σ (C5 - C7) and the bonding donor π* (C10 - C12). NBO calculations indicate that the host/guest complex is stabilized through interactions among the carbon molecules and the transfer of charge between occupied and unoccupied orbitals within the complex. Notably, the highest hyperconjugative E (2) energy is observed during these intermolecular interactions, underscoring their significance in potential medicinal and biological applications [33].

3.4 NLO Studies

Nonlinear optics (NLO) is the scientific discipline dedicated to exploring the interaction between light and matter. It encompasses a broad spectrum of phenomena, including light-by-light scattering, stimulated light scattering, same and difference frequency generation, intensity-dependent effects on physical properties like refractive index, and harmonic generation [34]. NLO technology holds significant promise for a multitude of industries, including photonics, optoelectronics, biomedicine, molecular switches, luminescent materials, laser technology, spectroscopic and electrochemical sensors, data storage, microfabrication, imaging, optical signal modulation, and telecommunications [35]. Density Functional Theory (DFT) holds immense potential for the analysis of NLO processes in metal alkynyl complexes, organic molecules, and the prediction of trends in initial hyperpolarizabilities for related complexes. It is expected to play a pivotal role in the advancement of NLO materials, both in the present and in the future [36].

Specifically, organic compounds with delocalized π-conjugated electronic systems hold great promise for NLO applications. These compounds can achieve substantial molecular hyperpolarizability through efficient charge transfer mechanisms facilitated by π-conjugated bridge frameworks and push-pull architectures [34].

The hyperpolarizability of serotonin is evaluated using the finite field methodology and the B3LYP/6-311++G(d,p) method. Computed parameters are presented in Table 4. Notably, the numbers α and β in the Gaussian output are originally provided in atomic units (a.u) and have been converted into electronic units (esu) (α; 1 a.u = 0.1482 10-24 esu, β; 1 a.u = 8.6393 10-33 esu). Relevant equations can be applied to determine essential values such as mean polarizability (α), anisotropy polarizability (Δα), and the average value of the first hyperpolarizability (β).

$$\alpha_{tot} = \frac{1}{3}(\alpha_{xx} + \alpha_{yy} + \alpha_{zz})$$

$$\Delta\alpha = \frac{1}{\sqrt{2}}[(\alpha_{xx} - \alpha_{yy})^2 + (\alpha_{yy} - \alpha_{zz})^2 + (\alpha_{zz} - \alpha_{xx})^2 + 6\alpha_{xz}^2 + 6\alpha_{xy}^2 + 6\alpha_{yz}^2]^{1/2}$$

$$\beta_{TOTAL} = (\beta_x^2 + \beta_y^2 + \beta_z^2)^{1/2}$$

Where, $\beta_x = \beta_{xxx} + \beta_{xyy} + \beta_{xzz}$;

$\beta_y = \beta_{yyy} + \beta_{yzz} + \beta_{yxx}$;

$\beta_z = \beta_{zzz} + \beta_{zxx} + \beta_{zyy}$;

From the dipole moment values the total dipole moment is given by

$\mu = (\mu_x^2 + \mu_y^2 + \mu_z^2)^{1/2}$ [31 - 34].

Table 4 (a) Dipole moment, mean polarizabity, the anisotropic of the polarizability and the mean first-order hyperpolarizability values obtained using DFT Analysis

Dipole (Debye)		Polarizability a.u		Hyperpolarizability a.u	
μ_x	-0.7500	α_{xx}	-87.0200	β_{xxx}	30.7204
μ_y	0.9780	α_{xy}	8.9837	β_{xxy}	11.1365
μ_z	0.5256	α_{yy}	-59.2042	β_{xyy}	-13.0213
μ	1.3399	α_{xz}	-1.9658	β_{yyy}	7.5866
		α_{yz}	2.4382	β_{xxz}	21.5444
		α_{zz}	-81.1360	β_{xyz}	7.7131
				β_{yyz}	-1.3143
				β_{xzz}	-11.0243
				β_{yzz}	-8.1640
				β_{zzz}	2.3333

Table 4 (b) Calculated NLO Parameters

Parameters	Values(esu)
α_{tot}	1.3399
$\Delta\alpha$	2.54 x10^{-23}
β_{tot}	2.068x10^{-31}

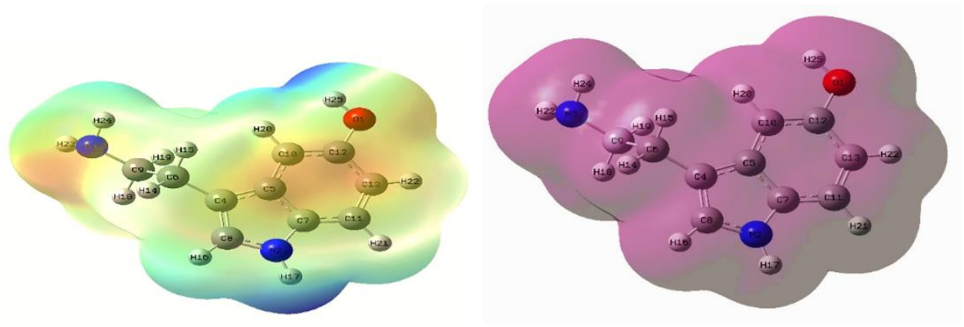

(a) MESP & MTED surface

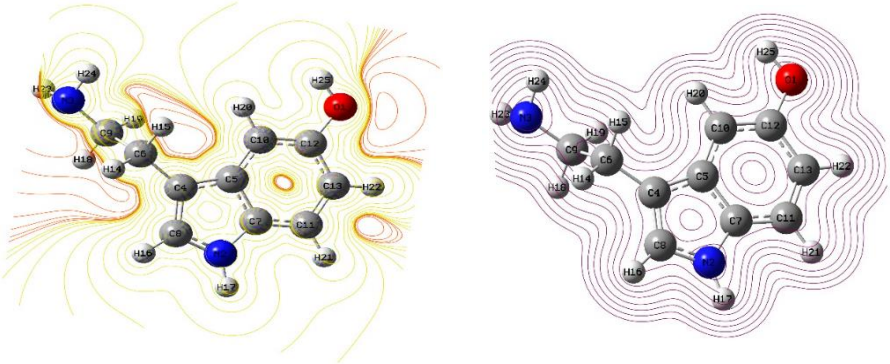

(b) CESP & CTED Suface

Figure 4. Molecular Electrostatic Potential Surfaces

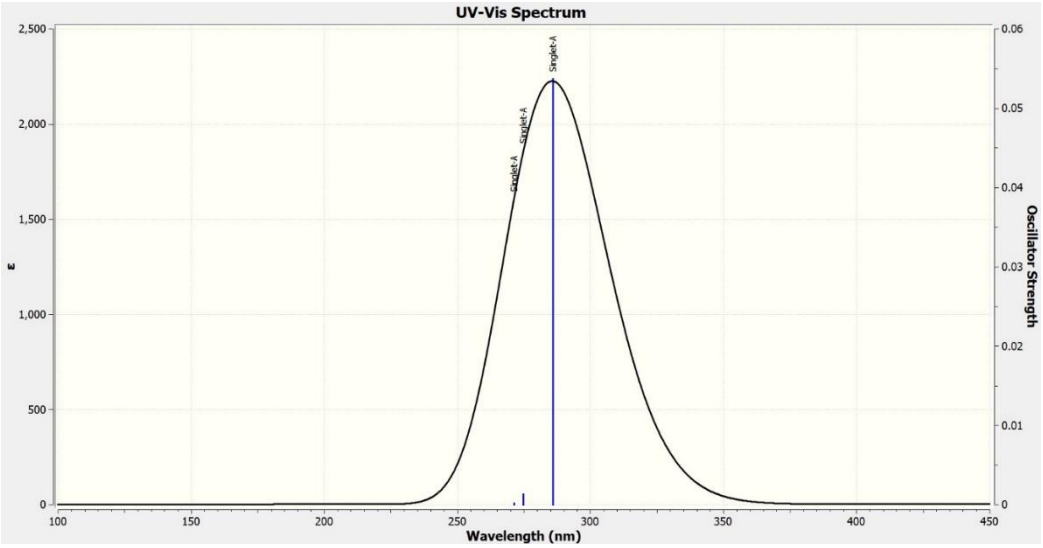

Figure 5. The excitation spectrum of Serotonin

Table 5 The calculated values of Excitation energies, Absorption wavelength and Oscillator strengths

Excited state	Excitation energies (eV)	Absorption wavelength λ(nm)	Oscillator strengths(f)
E.S-1	0.0537eV	285.98 nm	96522.60
E.S-2	0.0013 eV	274.73 nm	2336.67
E.S-3	0.0002 eV	271.21nm	359.488

The calculated dipole moment (μ) of the molecule measures 1.3399 Debye. In the realm of nonlinear optics (NLO), the magnitude of the molecular hyperpolarizability (β) is a critical factor. Serotonin exhibits a total initial hyperpolarizability value (β tot) of

222.81265 x 10-33 esu. All the calculated values are listed in Table 4 a & b.

When investigating nonlinear optical properties, urea and p-nitroaniline (p-NA) molecules serve as common reference systems. For instance, urea possesses an initial hyperpolarizability of approximately 0.2 x 10-30 esu and an electric dipole moment of 1.373 D [37]. Remarkably, the dipole moment and initial hyperpolarizability values of the serotonin molecule closely align with those observed for the reference compound. It is well-established that higher values of dipole moment, molecular polarizability, and hyperpolarizability are key attributes contributing to enhanced NLO properties in a molecular system [11].

3.5 Mapped surface / Contour surface of ESP and TED

The concept of Molecular Electrostatic Potential (MESP) is often represented through a color-coded visualization, which serves to highlight regions of varying charge within a molecule. This visualization technique is instrumental in assessing the molecule's susceptibility to electrophilic and nucleophilic attacks [38,39]. By utilizing color gradations, it offers simultaneous insights into the molecule's size, structure, and the distribution of positive, negative, and neutral electrostatic potential regions [39, 40] Furthermore, MESP proves highly valuable for exploring the relationship between molecular structure and physicochemical properties, as well as for predicting the behavior of intricate molecules and intermolecular interactions [40].

To illustrate this concept, we generated contour maps depicting the total electron density and electrostatic potential surfaces of serotonin (Figure 4). In these maps, regions that are moderately electron-rich or bear a partial negative charge are visualized in red, while areas exhibiting slight electron deficiency or a positive charge are indicated by shades of blue, light blue, and yellow, respectively [38]. In this representation, zones with lower potential are denoted in red, signifying an abundance of electrons, whereas those with higher potential are depicted in blue, indicating a relative scarcity of electrons.

The MESP surface for serotonin clearly reveals a region with a small electrostatic potential energy surrounding the phenyl group and the N-H bond, which is colored in a slightly yellowish-orange hue, while red is notably absent. This observation suggests that the atoms within the phenyl ring and the N-H (N3-H23) bond may possess the smallest electrostatic energy compared to other atoms. Conversely, the O-H and N-H (N2-H17) bonds, represented in blue, exhibit a substantial electrostatic potential energy, whereas the remainder of the molecule appears nearly neutral. Hydrogen atoms (H17 and H25), primarily encircled by blue regions, are probable sites for nucleophilic attacks due to their positive electrostatic potential, as indicated by the MESP analysis. Conversely, atoms within the phenyl group, largely enveloped in orange hues stemming from the prevalence of negative electrostatic potential, may be susceptible to electrophilic attacks.

Additionally, as depicted in Figure 4 the mapped Total Electron Density (TED) surface, considering the electron density offers a more comprehensive understanding of the molecule's size. The contour maps on this surface provide valuable information about the molecule's reactive regions [17].

3.6 Optical Studies

Time-Dependent Density Functional Theory (TD-DFT) approaches offer precise theoretical calculations of ground and excited state properties for organic electronic materials [41, 42]. To comprehensively investigate electronic transitions, it is essential to consider the lowest singlet-singlet allowed excited states [43]. In our current research, we applied the TD-DFT/B3LYP/6-311++G(d,p) method to determine maximum excitation energies (E) in electronvolts (eV), oscillator strengths (f) in atomic units (a.u), and absorption wavelengths (λ) in nanometers (nm) for the molecules in their gaseous phase. The excitation spectrum is depicted in Figure 5. Table 5 listed the calculated values for title molecule Serotonin.

The observed peaks in the spectrum primarily arise from one-electron excitations, particularly those involving HOMO-LUMO, HOMO-1 LUMO, and HOMO-2 LUMO. Table 5 lists the three excited states' resulting excited energies, wavelengths, and oscillator strengths. Based on the calculated excited state values, it becomes evident that as the absorption wavelength decreases, the oscillator strength also decreases proportionally.

4. Conclusion

To ascertain the structural attributes, HOMO-LUMO energy levels, NBO analysis, MEP, and NLO activity of the molecule, ab initio and DFT simulations were employed. The molecular geometry was optimized using the DFT/B3LYP approach with a 6-311++G basis set. The most significant charge transfer occurring within the molecule was identified by examining the interactions between HOMO and LUMO orbitals. Additionally, NBO analysis was employed to investigate the molecule's stability, examining hyper conjugative interactions and charge delocalization. Through Nonlinear Optical (NLO) studies, it was established that a significant neurotransmitter like serotonin exhibits favourable NLO properties. Excited state energies were computed via UV studies using TD-DFT, leading to the observation that as excited states increase, excited energies decrease. The molecule's electrophilic and nucleophilic tendencies were investigated using MESP and MTED analyses.

References

[1] L.F. Mohammad-Zadeh, L. Moses, S.M. Gwaltney-Brant, Serotonin: a review. Journal of Veterinary Pharmacology and Therapeutics, 31(3), (2008) 187–199. https://doi.org/10.1111/j.1365-2885.2008.00944.x

[2] M.A. Geyer, & F.X. Vollenweider, Serotonin research: contributions to understanding psychoses. Trends in pharmacological sciences, 29(9), 2008) 445-453. https://doi.org/10.1016/j.tips.2008.06.006

[3] M. Paulmichl, F. Friedrich, E. Woll, H. Weiss, F. Lang, Effects of serotonin on electrical properties of Madin-Darby canine kidney cells. Pflugers Archiv, 411, (1988) 394-400. https://doi.org/10.1007/BF00587718

[4] S. K. Kaushalya, Suman Nag, J. Balaji, S. Maiti, Serotonin: Multiphoton Imaging and Relevant Spectral Data. Multiphoton Microscopy in the Biomedical Sciences VIII, 6860, (2008) 223-230. https://doi.org/10.1117/12.763020

[5] H.A. Lechner, D.A. Baxter, J.W. Clark, J.H. Byrne, Bistability and Its Regulation by Serotonin in the Endogenously Bursting Neuron Rl5 in Aplysia, Journal of neurophysiology, 75(2), (1996) 957-962. https://doi.org/10.1152/jn.1996.75.2.957

[6] J. Best, H.F. Nijhout, M. Reed, Serotonin synthesis, release and reuptake in terminals: a mathematical model. Theoretical Biology and Medical Modelling, 7, (2010) 1-26. https://doi.org/10.1186/1742-4682-7-34

[7] C. Cabezas, M. Varela, I. Pena, J.C. Lopez, J.L. Alonso, The microwave spectrum of neurotransmitter serotonin. Physical Chemistry Chemical Physics, 14(39), (2012) 13618-13623. https://doi.org/10.1039/C2CP42654D

[8] N. Schweighofer, S.C. Tanaka, K. Doya, Serotonin and the evaluation of future rewards: theory, experiments, and possible neural mechanisms. Annals of the New York Academy of Sciences, 1104(1), (2007) 289-300. https://doi.org/10.1196/annals.1390.011

[9] K.W. Kaufmann, E.S. Dawson, L.K. Henry, J.R. Field, R.D. Blakely, J. Meiler, Structural determinants of species-selective substrate recognition in human and Drosophila serotonin transporters revealed through computational docking studies. Proteins: Structure, Function, and Bioinformatics, 74(3), (2009) 630-642. https://doi.org/10.1002/prot.22178

[10] A. Joshi, D.H. Wang, S. Watterson, P.L. McClean, C.K. Behera, T. Sharp, K. Wong-Lin, Opportunities for multiscale computational modelling of serotonergic drug effects in Alzheimer's disease. Neuropharmacology, 174, (2020) 108118. https://doi.org/10.1016/j.neuropharm.2020.108118

[11] S. Krishna Priya, R. Karunathan, E. Shobhana, B. Babu, R. Kesavasamy, S. Akila, M. Karpagavalli, A quantum chemical analysis of an organic compound: 3,5- bis (4-hydroxy phenyl)-2,4,6-trimethyl cyclohexanone, AIP Conference Proceedings 2446, (2022) https://doi.org/10.1063/5.0108265

[12] F.S. Manciu, J. D. Ciubuc, E.M. Sundin, C. Qiu, K.E. Bennet, Analysis of Serotonin Molecules on Silver Nanocolloids—A Raman Computational and Experimental Study. Sensors, 17(7), (2017) 1471. https://doi.org/10.3390/s17071471

[13] A. Prah, M. Purg, J. Stare, R.Vianello, J. Mavri,. How monoamine oxidase A decomposes serotonin: an empirical valence bond simulation of the reactive step. The Journal of Physical Chemistry B, 124(38), (2020) 8259-8265. https://doi.org/10.1021/acs.jpcb.0c06502

[14] M.C. Reed, H.F. Nijhout, J. Best, (2013). Computational studies of the role of serotonin in the basal ganglia. Frontiers in Integrative Neuroscience, 7, 41. https://doi.org/10.3389/fnint.2013.00041

[15] A. Rathore, V. Asati, M. Mishra, R. Das, V. Kashaw, S.K. Kashaw, Computational approaches for the design of novel dopamine D2 and serotonin 5-HT2A receptor dual antagonist towards schizophrenia. In Silico Pharmacology, 10(1), (2022) 7. https://doi.org/10.1007/s40203-022-00121-5

[16] T. Zeppelin, L.K. Ladefoged, S. Sinning, B. Schiøtt, Substrate and inhibitor binding to the serotonin transporter: Insights from computational, crystallographic, and functional studies. Neuropharmacology, 161 (2019) 107548. https://doi.org/10.1016/j.neuropharm.2019.02.030

[17] N.S. Yaakob, D.T. Nguyen, B. Exintaris, H.R. Irving, The C and E subunits of the serotonin 5-HT3 receptor subtly modulate electrical properties of the receptor. Biomedicine & Pharmacotherapy, 97, (2018) 1701-1709. https://doi.org/10.1016/j.biopha.2017.12.010

[18] S. Sevvanthi, S. Muthu, S. Aayisha, P. Ramesh, M. Raja, Spectroscopic (FT-IR, FT-Raman and UV-Vis), computational (ELF, LOL, NBO, HOMO-LUMO, Fukui, MEP) studies and molecular docking on benzodiazepine derivatives-heterocyclic organic arenes. Chemical Data

Collections, 30, (2020) 100574, https://doi.org/10.1016/j.cdc.2020.100574

[19] H. Safia, L. Ismahan, G. Abdelkrim, C. Mouna, N. Leila, M. Fatiha, Density functional theories study of the interactions between host β-Cyclodextrin and guest 8-Anilinonaphthalene-1-sulfonate: Molecular structure, HOMO, LUMO, NBO, QTAIM and NMR analyses. Journal of Molecular Liquids, 280, (2019) 218-229. https://doi.org/10.1016/j.molliq.2019.01.019

[20] M. Buvaneswari, R. Santhakumari, C. Usha, R. Jayasree, Suresh Sagadevan, Synthesis, growth, structural, spectroscopic, optical, thermal, DFT, HOMO–LUMO, MEP, NBO analysis and thermodynamic properties of vanillin isonicotinic hydrazide single crystal, Journal of Molecular Structure, 1243 (2021), 130856. https://doi.org/10.1016/j.molstruc.2021.130856

[21] F. Basha, F.L.A. Khan, S. Muthu, M. Raja, Computational evaluation on molecular structure (Monomer, Dimer), RDG, ELF, electronic (HOMO-LUMO, MEP) properties, and spectroscopic profiling of 8-Quinolinesulfonamide with molecular docking studies. Computational and Theoretical Chemistry, 1198, (2021)113169. https://doi.org/10.1016/j.comptc.2021.113169

[22] M.A. Mumit, T.K. Pal, M.A. Alam, M.A.A.A.A. Islam, S. Paul, M.C. Sheikh, DFT studies on vibrational and electronic spectra, HOMO–LUMO, MEP, HOMA, NBO and molecular docking analysis of benzyl-3-N-(2, 4, 5-trimethoxyphenylmethylene) hydrazinecarbodithioate. Journal of molecular structure, 1220, (2020) 128715. https://doi.org/10.1016/j.molstruc.2020.128715

[23] A. Dwivedi, A. Kumar, Molecular Docking and Comparative Vibrational Spectroscopic Analysis, HOMO-LUMO, Polarizabilities, and Hyperpolarizabilities of N-(4- Bromophenyl)-4-Nitrobenzamide by Different DFT (B3LYP, B3PW91, and MPW1PW91) Methods. Polycyclic Aromatic Compounds, 41(2), (2021) 387-399. https://doi.org/10.1080/10406638.2019.1591466

[24] V. Anbu, R. Karunathan, K.A. Vijayalakshmi, A. David Stephen, P.V. Nidhin, Explosives properties of high energetic Trinitrophenyl Nitramide molecules: A DFT and AIM analysis, Arabian Journal of Chemistry, 12(5), (2019) 621-632. https://doi.org/10.1016/j.arabjc.2016.09.023

[25] T. Karthick, V. Balachandran, S. Perumal, A. Nataraj, Rotational isomers, vibrational assignments, HOMO–LUMO, NLO properties and molecular electrostatic potential surface of N-(2 bromoethyl) phthalimide, Journal of Molecular Structure, 1005 (2011) 202–213, https://doi.org/10.1016/j.molstruc.2011.08.051

[26] S. Aslam, M. Haroon, T. Akhtar, M. Arshad, M. Khalid, Z. Shafiq, M. Imran, Ullah, A. Synthesis, Characterization, and DFT-Based Electronic and Nonlinear Optical Properties of Methyl 1 - (arylsulfonyl)-2-aryl-1Hbenzo[d]imidazole-6-carboxylates, American Chemical Society, 7(35), (2022) 31036-31046.

[27] M. Miar, A. Shiroudi, K. Pourshamsian, A.R. Oliaey, F. Hatamjafari, Theoretical investigations on the HOMO–LUMO gap and global reactivity descriptor studies, natural bond orbital, and nucleus-independent chemical shifts analyses of 3-phenylbenzo [d] thiazole-2 (3 H)-imine and its para-substituted derivatives: Solvent and substituent effects. Journal of Chemical Research, 45(1-2), (2021) 147-158. https://doi.org/10.1177/1747519820932091

[28] N. Choudhary, S. Bee, A. Gupta, P. Tandon, Comparative vibrational spectroscopic studies, HOMO–LUMO and NBO analysis of N-(phenyl)-2, 2-dichloroacetamide, N-(2-chloro phenyl)-2, 2-dichloroacetamide and N-(4-chloro phenyl)-2, 2-dichloroacetamide based on density functional theory. Computational and Theoretical Chemistry, 1016, (2013) 8-21. https://doi.org/10.1016/j.comptc.2013.04.008

[29] H. AlRabiah, S. Muthu, F. Al-Omary, A.M. Al-Tamimi, M. Raja, R.R.Muhamed, A.A.R. El-Emam, Molecular structure, vibrational spectra, NBO, Fukui function, HOMO-LUMO analysis and molecular docking study of 6-[(2-methylphenyl) sulfanyl]-5-propylpyrimidine-2, 4 (1H, 3H)-dione. Macedonian Journal of Chemistry and Chemical Engineering, 36(1), (2017) 59-80. https://doi.org/10.20450/mjcce.2017.1001

[30] B.F. Rizwana, J.C. Prasana, S. Muthu, C.S. Abraham, Spectroscopic (FT-IR, FT-Raman, NMR) investigation on 2-[(2-amino-6-oxo-6, 9-dihydro-3H-purin-9-yl) methoxy] ethyl (2S)-2-amino-3-methylbutanoate by Density Functional Theory. Materials Today: Proceedings, 18, (2019) 1770-1782. https://doi.org/10.1016/j.matpr.2019.05.276

[31] V. Mohanraj, P. Sakthivel, S. Ponnuswamy, P. Muthuraja, M. Dhandapani, Growth, spectral, thermal, NLO studies and computational studies on novel NLO organic crystals of N-Nitroso-r-2, c-6-bis (4-methoxyphenyl)-t-3-ethyl-piperidin-4-one. Materials Today: Proceedings, 8, (2019) 1-10. https://doi.org/10.1016/j.matpr.2019.02.074

[32] R. Sreedharan, S. Ravi, K.R. Raghi, T.M. Kumar, K. Naseema, Growth, linear-nonlinear optical studies and quantum chemistry formalism on an

organic NLO crystal for opto-electronic applications: experimental and theoretical approach. SN Applied Sciences, 2, (2020) 1-18. https://doi.org/10.1007/s42452-020-2360-9

[33] N. Arif, Z. Shafiq, S. Noureen, M. Khalid, A. Ashraf, M. Yaqub, S.R. Al-Mhyawi, Synthesis, spectroscopic, SC-XRD/DFT and non-linear optical (NLO) properties of chromene derivatives. RSC advances, 13(1), (2023) 464-477. https://doi.org/10.1039/D2RA07134G

[34] S. Munsif, S. Khan, A. Ali, M.A. Gilani, J. Iqbal, R. Ludwig, K. Ayub, Remarkable nonlinear optical response of alkali metal doped aluminum phosphide and boron phosphide nanoclusters. Journal of Molecular Liquids, 271 (2018) 51-64. https://doi.org/10.1016/j.molliq.2018.08.121

[35] N. Karthikeyan, J. Joseph Prince, S. Ramalingam, S. Periandy, Electronic [UV-Visible] and vibrational [FT-IR, FT-Raman] investigation and NMR - Mass spectroscopic analysis of Terephthalic acid using quantum Gaussian calculations. Spectrochimica Acta Part A: Molecular and Biomolecular Spectroscopy, 139, (2015) 229-242. http://dx.doi.org/10.1016/j.saa.2014.11.112

[36] M.S. Kodikara, R. Stranger, M.G. Humphrey, Computational studies of the nonlinear optical properties of organometallic complexes. Coordination Chemistry Reviews, 375, (2018) 389-409. https://doi.org/10.1016/j.ccr.2018.02.007

[37] H. Abbas, M. Shkir, S. AlFaify, Density functional study of spectroscopy, electronic structure, linear and nonlinear optical properties of l-proline lithium chloride and l-proline lithium bromide monohydrate: For laser applications. Arabian Journal of Chemistry, 12(8), (2019) 2336-2346. https://doi.org/10.1016/j.arabjc.2015.02.011

[38] S. Sambandam, B. Sarangapani, S. Paramasivam, R. Chinnaiyan, Molecular structure, vibrational spectral investigations (FT-IR and FT-Raman), NLO, NBO, HOMO-LUMO, MEP analysis of (E)-2-(3-pentyl-2, 6-diphenylpiperidin-4-ylidene)-N-phenylhydrazinecarbothioamide based on DFT and molecular docking studies. Biointerface Research in Applied Chemistry, 11 (2021) 11833-11855. https://doi.org/10.33263/BRIAC114.1183311855

[39] C. Karnan, K.S. Nagaraja, S. Manivannan, A. Manikandan, V. Ragavendran, Crystal structure, spectral investigations, DFT and antimicrobial activity of brucinium benzilate (BBA). Journal of Molecular Modeling, 27, (2021) 1-11. https://doi.org/10.21203/rs.3.rs-343924/v1

[40] T. Dey, K.S.S. Praveena, S. Pal, A.K. Mukherjee, three oxime ether derivatives: Synthesis, crystallographic study, electronic structure and molecular electrostatic potential calculation. Journal of Molecular Structure, 1137, (2017) 615-625. https://doi.org/10.1016/j.molstruc.2017.02.089

[41] R. Zaier, S. Hajaji, M. Kozaki, S. Ayachi, DFT and TD-DFT studies on the electronic and optical properties of linear π-conjugated cyclopentadithiophene (CPDT) dimer for efficient blue OLED. Optical Materials, 91, (2019) 108-114. https://doi.org/10.1016/j.optmat.2019.03.013

[42] H. Kargar, R. Behjatmanesh-Ardakani, V. Torabi, M. Kashani, Z. Chavoshpour-Natanzi, Z. Kazemi, V. Mirkhani, A. Sahraei, M.N. Tahir, M. Ashfaq, K.S. Munawar, Synthesis, characterization, crystal structures, DFT, TD-DFT, molecular docking and DNA binding studies of novel copper(II) and zinc(II) complexes bearing halogenated bidentate N,O-donor Schiff base ligands. Polyhedron, 195, (2021) 114988. https://doi.org/10.1016/j.poly.2020.114988

[43] S. Bibi, F. Farooq, F.Q. Bai, H.X. Zhang, DFT and TD-DFT studies of phenothiazine based derivatives as fluorescent materials for semiconductor applications, Shamsa Bibi, Faiza Farooq, Shafiq-ur-Rehman, Fu Quan Bai, Hong-Xing Zhang, Materials Science in Semiconductor Processing, 134, (2021) 106036. https://doi.org/10.1016/j.mssp.2021.106036

Has this article screened for similarity?

Yes

Authors Contribution Statement

R. Thayala Sanker - Methodology, Formal analysis, Investigation, Writing Original Draft; **Arunachalam** S – Data curation, Investigation, Supervision, Visualization, Validation, Writing –Review & Editing, **S. Raju**- Writing – Review & Editing; **M. Velayutham Pillai** - Writing – Review & Editing; **R. Kumaresan** - Writing –Review & Editing. All the authors read and approved the final version of the manuscript.

Conflict of Interest

The Authors have no conflicts of interest on this article to declare.

About the License